Chinese Chemical Letters 34 (2023) 107769

Contents lists available at ScienceDirect

Chinese Chemical Letters

journal homepage: www.elsevier.com/locate/cclet

Promotion effect of bulk sulfates over CeO_2 for selective catalytic reduction of NO by NH_3 at high temperatures

Jiawei Ji[a], Li Han[a], Wang Song[a], Jingfang Sun[d], Weixin Zou[b,*], Changjin Tang[c,*], Lin Dong[a,b,d]

[a] Laboratory of Mesoscopic Chemistry of MOE, School of Chemistry and Chemical Engineering, Nanjing University, Nanjing 210023, China
[b] School of the Environment, Nanjing University, Nanjing 210023, China
[c] School of Environment, Nanjing Normal University, Nanjing 210023, China
[d] Jiangsu Key Laboratory of Vehicle Emission Control, Center of Modern Analysis, Nanjing University, Nanjing 210023, China

ARTICLE INFO

Article history:
Received 16 May 2022
Revised 4 August 2022
Accepted 21 August 2022
Available online 23 August 2022

Keywords:
NH_3-SCR
CeO_2
Bulk sulfates
High temperature denitration
NH_3 adsorption
NH_3 oxidation

ABSTRACT

Understanding the influence of sulfates over catalysts for selective catalytic reduction of NO with NH_3 (NH_3-SCR) is crucial due to the universal presence of SO_2 in exhaust gas. Depending on the degree of sulfation, there mainly exist surface and bulk sulfates and NH_3-SCR activity is generally considered to suffer more from bulk sulfates. Herein, the unique function of bulk sulfates over CeO_2 in promoting high-temperature SCR reaction is revealed. Notably, compared with CeO_2 dominated with surface sulfates (S-CeO_2–4h) and commercial V_2O_5-WO_3/TiO_2, CeO_2 with bulk sulfates (S-CeO_2–72h) exhibits admirable NO conversion at the temperature range of 400–550 °C. Bulk sulfates provide more Brønsted acid sites with stronger strength for NH_3 adsorption. Moreover, the oxidation ability of CeO_2 is significantly inhibited due to electron-withdrawing effect from bulk sulfates, which alleviates NH_3 oxidation at high temperatures. More NH_3 adsorption with high stability and limited NH_3 oxidation capacity ensure the excellent catalytic performance for S-CeO_2–72h in high-temperature denitration. This work provides new insight of bulk sulfates in promoting SCR activity and open a new avenue to design deNO_x catalysts employed at high temperatures.

Nitrogen oxides composed of NO and NO_2 (NO_x) are one of the major air pollutants. Selective catalytic reduction of NO by NH_3 (NH_3-SCR) over V_2O_5-WO_3(MoO_3)/TiO_2 is currently the most effective method for treating exhausts from stationary sources like thermal power plants [1,2]. However, vanadia-based catalysts still suffer from a narrow temperature window (300–400 °C), undesirable N_2O products at high temperatures, and toxic properties of VO_x. As a consequence, it is of great urgency to develop vanadia-free catalysts with excellent catalytic performance [3–5]. Over the past decades, CeO_2-based catalysts have demonstrated remarkable catalytic performance for NH_3-SCR reaction and can be a prime candidate for traditional V_2O_5-WO_3/TiO_2 [6–9].

It is unavoidable for the exhaust from stationary sources to contain a certain amount of sulfur species. Generally, sulfur poisoning is one of the major factors causing catalyst deactivation [10–13]. In recent years, various literatures have shown that SO_2 can facilitate the sulfate formation over catalyst and then promote NH_3-SCR reaction rate in the medium temperature range (250–350 °C), especially for CeO_2-based catalysts [14–17]. Gu *et al.* first discover the unusual phenomenon that the activity of CeO_2 was greatly improved after SO_2 pretreatment [18]. Yang *et al.* found that the enhanced acidity and Eley-Rideal mechanism were the main reason for activity promotion [19]. Subsequently, the sulfation of CeO_2 with different morphology was explored and the presence of separate reaction sites for NH_3 (surface sulfates) and NO_x (Ce^{4+}) was important for the improvement of SCR reaction [17,20]. Zhang *et al.* found that high temperature would promote the diffusion of sulfates from surface to the bulk phase of CeO_2 and formed bulk sulfates could inhibit the SCR activity, which could be effectively alleviated by surface Ti modification [21,22].

As a summary, depending on the degree of sulfation, there mainly exist surface and bulk sulfates. Surface sulfates are mainly formed at low operation temperature or for short periods of time. With the temperature elevating or treatment duration increasing, the formed sulfates can be further accumulated and crystallized to form bulk sulfates [23–26]. And it is generally believed that the surface sulfates (acid sites) can synergistically interact with the surface redox sites (metal sites) to promote SCR reaction.

* Corresponding authors.
E-mail addresses: wxzou2016@nju.edu.cn (W. Zou), tangcj@njnu.edu.cn (C. Tang).

https://doi.org/10.1016/j.cclet.2022.107769
1001-8417/

However, the formation of bulk sulfates can greatly weaken the redox ability of catalysts, resulting in the further reduction of catalytic activity [16,22,27,28]. Herein, the unique function of bulk sulfates in high-temperature SCR reaction is explored. CeO_2 with bulk sulfates obtained by long-term sulfation displayed much better SCR activity at high temperatures (400–550 °C) than surface sulfates modified CeO_2 and even commercial V_2O_5-WO_3/TiO_2. *Via* various characterizations including Ar ion sputtering XPS, it is proposed the enhanced NH_3 adsorption and reduced NH_3 oxidation capacity provided by bulk sulfates are the main reason to ensure high activity at high temperatures. The role of bulk sulfates in catalytic reduction of NO is well revealed.

Breakthrough experiment is carried out to study the adsorption behavior of SO_2 on CeO_2 (Fig. 1a). In a previous work, we have studied the effect of sulfation temperature on the nature of sulfate species over CeO_2. It was found bulk sulfates were dominated when the temperature was higher than 300 °C and at temperature as low as 150 °C, there mainly formed surface sulfates [21]. Additional study showed under the stream of 1000 ppm $SO_2 + 5\%$ O_2, CeO_2 surface can be fully covered with sulfates after 4 h sulfation process [29]. Here, it is evident from the SO_2-breakthrough curve that the sulfation process can be divided into three stages. In the first 4 h, the signal of outlet SO_2 increases rapidly, followed by a slowdown of adsorption process over the next 20 h. Unexpectedly, as time continues to increase to 72 h, SO_2 can still be adsorbed slowly, revealing the absence of saturation adsorption. To further confirm this point, TG is employed to estimate the amount of deposited sulfate species (Fig. S1 and Table S1 in Supporting information). It is found that with the extension of sulfation duration, the amount of sulfate species increases from 3.92% (4 h) to 6.87% (24 h) and 8.72% (72 h), respectively. The results proves that accumulated adsorption of SO_2 on ceria is occurred. To further explore the influence of sulfation time on the type of sulfate species, 4, 24, and 72 h are chosen as the time length of sulfation, and the obtained samples are labeled as S-CeO_2-*x*h (*x* = 4, 24, and 72).

ATR-IR is employed to determine the nature of sulfates and the result is shown in Fig. 1b. For original CeO_2, the bands at 1313 cm^{-1} and 1055 cm^{-1} can be attributed to the stretching vibration of Ce-O-Ce. After the treatment under $SO_2 + O_2$, two peaks at 1116 cm^{-1} and 1050 cm^{-1} emerge and they can be assigned to surface sulfates. With the extension of sulfation time to 24 h and 72 h, a new band at 995 cm^{-1} emerges, which can be ascribed to bulk or bulk-like sulfates [25,30]. This demonstrates that SO_2 does indeed experiences a permeation into the bulk of ceria as processing time increases, which is also confirmed by the gradual increase of H_2-TPR reduction temperature (Fig. S2 in Supporting information). XRD characterization gives further direct evidence. As can be seen in Fig. 1c, the diffraction peaks at $2\theta = 28.5°$, 33.1°, 47.6° and 56.4° typical of (111), (200), (220) and (311) lattice plane for cubic fluorite CeO_2 (PDF-ICDD 34–0394) are apparent. For S-CeO_2–4h, there was no significant change in peak strength and surface sulfates have little effect on the bulk phase structure of CeO_2. However, with the increasing of sulfation time, the reduction of main peak at 28.5° is detected, suggesting the sulfation treatment introduces some disturbance to the fluorite structure of CeO_2 (embedded graph in Fig. 1c). Moreover, for S-CeO_2–72h, there appears a peak at 20.1°, which can be assigned to the diffraction peak of $Ce_2(SO_4)_3$ (Fig. S3 in Supporting information) [21,31]. Thus, it is safely concluded that there mainly exist surface sulfates in S-CeO_2–4h sample, while bulk sulfates dominate in S-CeO_2–72h.

The catalytic performances in terms of NO conversion and N_2 selectivity over fresh and sulfated catalysts are displayed in Fig. 2. In line with the previous study, original CeO_2 shows quite poor activity and NO conversion reaches the highest of 50% at 350 °C due to a lack of acid sites [18,19]. The absence of a consecutive activity increment at temperature higher than 350 °C is assumed to be associated with NH_3 oxidation, which competes with NH_3 for SCR reaction [3], and this is also supported by the decreasing N_2 selectivity at higher temperatures (Fig. 2a). As for sulfated CeO_2, drastic enhancements in NO conversion and N_2 selectivity are observed. S-CeO_2–4h shows a volcanic profile. More than 80% NO can be converted at 250 °C, but the activity starts to decrease when the temperature is higher than 300 °C. With the deepening of sulfation process, the medium-temperature activity of sulfated CeO_2 gradually decreases. As a sharp comparison, the high-temperature NO conversion increases obviously. S-CeO_2–72h achieves poor SCR activity of less than 40% at temperature as low as 250 °C, even worse than that of pristine CeO_2. Nevertheless, it exhibits NO conversion of more than 80% in the temperature range of 400–550 °C, where the corresponding value is lower than 80% for S-CeO_2–4h. Commercial V_2O_5-WO_3/TiO_2 is also tested for comparison (the composition is presented in Table S2 in Supporting information) and it fares even worse with NO conversion of only 60% (Fig. 2b and Fig. S4 in Supporting information). Compared with the catalytic performance reported in literatures (Table S3 in Supporting information), S-CeO_2–72h with bulk sulfates also shows good competitiveness. Considering that the sulfation degree and catalytic performance of CeO_2 pretreated with 24 h are in the middle position between that

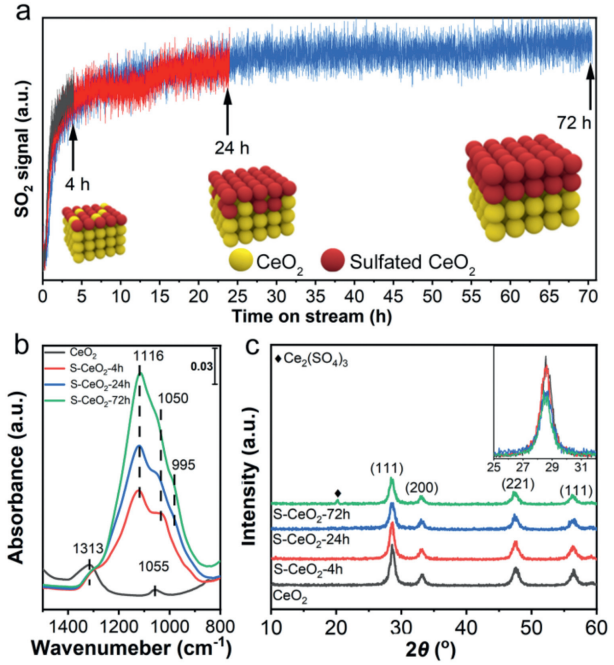

Fig. 1. (a) SO_2 breakthrough profiles over CeO_2 at 150 °C for different durations; (b) ATR-IR and (c) XRD patterns of CeO_2 and sulfated CeO_2.

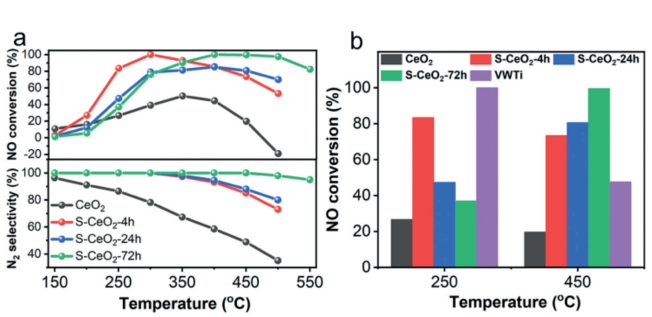

Fig. 2. (a) NO conversion and N_2 selectivity of CeO_2 and sulfated CeO_2 as a function of temperature, and (b) comparison of activity results with commercial V_2O_5-WO_3/TiO_2 at 250 °C and 450 °C, respectively. Reaction condition: 500 ppm NO, 500 ppm NH_3, 5% O_2, balanced with Ar, WHSV = 60,000 mL g^{-1} h^{-1}.

of 4 h and 72 h, S-CeO_2–4h with surface sulfates and S-CeO_2–72h with bulk sulfates are chosen for further study.

X-ray photoelectron spectra (XPS) are used to explore the surface electronic states of the catalysts. As presented in Figs. 3a and b, the spectra of S 2p of S-CeO_2–4h and S-CeO_2–72h mainly show hexavalent sulfate species, and no obvious signal from sulfites is found. The trend of S content changing with etching depth is further analyzed (Fig. 3c). S content of S-CeO_2–4h decreases sharply with increased etching, while S-CeO_2–72h with bulk sulfates exhibits a moderate decline. This result gives clear evidence that sulfates are gradually diffused into the bulk phase of CeO_2, which is in line with SO_2 breakthrough curve and XRD results. To explore the influence of embedded sulfur species, O 1s spectra are collected. SO_4^{2-} is a strong electron-withdrawing group, which can inhibit the redox ability of active centers [16]. In our previous work, we have found that the influence of SO_4^{2-} on CeO_2 can be reflected by the shift of lattice oxygen to higher binding energy [31]. As presented in Figs. 3d and e, the binding energy of lattice oxygen over S-CeO_2–72h (529.7 eV) is higher than that of S-CeO_2–4h (529.5 eV). Further analysis shows that with the increasing of etching depth, the binding energy of subsurface oxygen layers in S-CeO_2–4h decreases from 529.5 eV to 529.1 eV. For comparison, S-CeO_2–72h exhibits almost no change, demonstrating that bulk sulfates have a more profound effect on CeO_2.

The redox property is one of the central factors to determine the activity of NH_3-SCR. NH_3 oxidation experiments are employed to study the influence of surface and bulk sulfates on the redox property of CeO_2 (Fig. 4a). Pristine CeO_2 exhibits remarkable NH_3 oxidation capacity. NH_3 starts to be oxidized at 300 °C, followed by a large NH_3 conversion of more than 90% at 450 °C. This demonstrates the presence of strong competition from NH_3 oxidation with catalytic reduction of NO at high temperatures, which is also supported by the poor N_2 selectivity in NH_3 oxidation (Fig. S5 in Supporting information) and SCR reaction test (Fig. 2a). After sulfation treatment, NH_3 oxidation reaction is inhibited to certain degrees. For S-CeO_2–4h with surface sulfates, NH_3 begins to react with O_2 at 350 °C. But it still acquires a considerable NH_3 conversion of 80% at 450 °C, demonstrating that surface sulfates have limited influence on the redox property of CeO_2. As a consequence, NH_3 oxidation still occurs to some extent under high temperatures, which leads to the degradation of NO conversion. For comparison, bulk sulfates significantly inhibit the redox ability of CeO_2. Remarkably, S-CeO_2–72h exhibits a much worse NH_3 oxidation capacity with less than 5% conversion at 450 °C. The slight competition reaction of NH_3 oxidation makes more NH_3 participate in the SCR reaction at high temperatures.

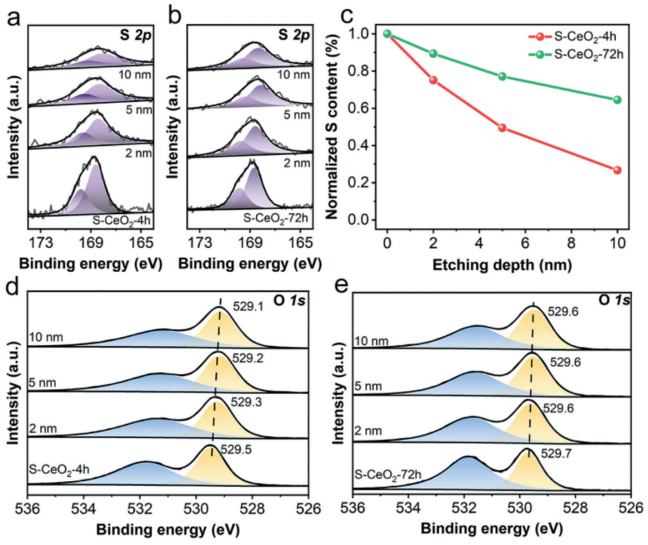

Fig. 3. Ion sputtering XPS of S 2p of (a) S-CeO_2–4h and (b) S-CeO_2–72h. (c) Normalized S content as a function of etching depth. Ion sputtering XPS of O 1s of (d) S-CeO_2–4h and (e) S-CeO_2–72h.

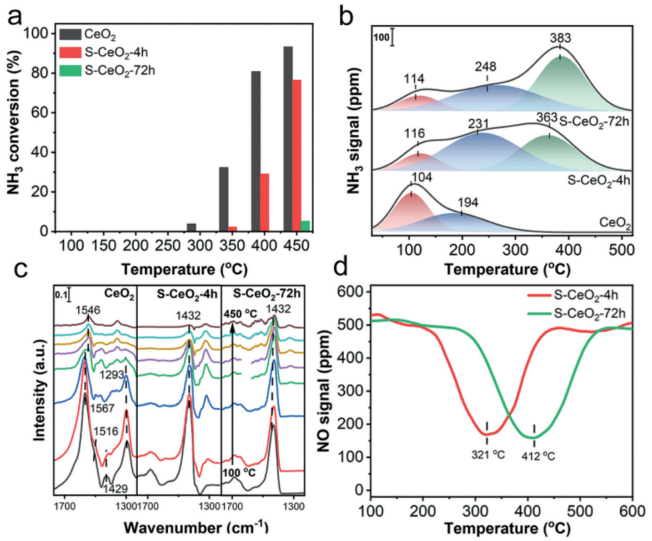

Fig. 4. (a) NH_3 oxidation, (b) NH_3-TPD, and (c) *in situ* DRIFTS of NH_3 adsorption over CeO_2, S-CeO_2–4h, and S-CeO_2–72h. (d) NO-TPSR of S-CeO_2–4h and S-CeO_2–72h.

The NH_3-adsorption stability of catalyst is an important factor to ensure SCR activity at high temperatures [19,32]. Thus, NH_3 temperature-programmed desorption (NH_3-TPD) is carried out to study the influence of different sulfates on acid properties, and the profiles along with integrated results are presented in Fig. 4b and Table S4 (Supporting information). It is notable that the amount and strength of NH_3 desorption are much stronger after SO_2+O_2 pretreatment, indicating both surface and bulk SO_4^{2-} can provide certain acid sites. For pristine CeO_2, two peaks at 104 °C and 194 °C with weak intensity emerge, which can be ascribed to physical/weak and moderate strength acid sites. As for sulfated samples, there appears a new desorption peak at high temperature, which belongs to the NH_3 adsorption on strong acid sites. The reduction of physically or weakly adsorbed acid sites may be related to the reduction of surface area after sulfation process (Table S4 in Supporting information). While for peaks of moderate and strong acid sites, it is worth noting that NH_3 desorption amount of S-CeO_2–72h at strong acid sites (0.157 mmol/g) increases a lot compared with that of S-CeO_2–4h (0.122 mmol/g). Moreover, the acid strength also exhibits an obvious enhancement with the peak shifting from 363 °C to 383 °C for S-CeO_2–72h, indicating that the bulk sulfates have stronger acidity and can adsorb NH_3 much more stably at a higher temperature.

In situ DRIFTS of NH_3 adsorption experiments are employed to distinguish the nature of surface acid sites (Fig. 4c). For pristine CeO_2, NH_3 adsorbed over both Lewis (1567 cm^{-1}, 1293 cm^{-1}) and Brønsted (1429 cm^{-1}) acid sites can be observed. It should be noticed that the peak at 1516 cm^{-1} belongs to –NH_2 species [17,19,31]. It mainly comes from the NH_3 dehydrogenation, which is closely related to the strong oxidation property of CeO_2. With the temperature rising, these peaks decrease sharply. NH_4^+ over Brønsted acid sites and activated -NH_2 almost vanish at 150 °C. Other NH_3 species over Lewis acid sites gradually disappear at 250 °C, in line with the result of NH_3-TPD. Further increment of temperature results in the appearance of nitrate species at 1536 cm^{-1} [17]. Notably, a significant change in acid type is observed for sulfated samples, where Lewis acid sites are negligible and only the signal attributed to Brønsted acid sites at 1423 cm^{-1} exists.

The only difference lies in the adsorption stability of NH_4^+species. The adsorbed NH_3 is almost completely desorbed over S-CeO_2–4h at 350 °C, while partial acid sites over S-CeO_2–72h retain NH_3 adsorption at 450 °C. These results indicate that NH_3 adsorption over bulk sulfates is much stronger and support the conclusion of NH_3-TPD.

Temperature programmed surface reaction (TPSR) is further carried out to investigate the reaction property of NH_3 adsorbed over surface and bulk sulfates. As presented in Fig. 4d, NO begins to react with adsorbed NH_3 at 200 °C and the largest reaction rate is achieved at 321 °C for S-CeO_2–4h. With further increase of temperature, NH_3 desorption and per-oxidation inevitably take place, resulting in restricted NO consumption at high temperatures. For S-CeO_2–72h, the weakened oxidation capacity makes it difficult for adsorbed NH_3 to participate in SCR reaction at low temperatures. And consequently, NH_3 begins to react at 300 °C, and acquires the maximum NO reaction rate above 400 °C, demonstrating enhanced NH_3 adsorption and restricted NH_3 oxidation promotes the reaction of NO with adsorbed NH_3 at high temperature.

Combined with TPSR and acidity/redox properties analysis, S-CeO_2–4h with surface sulfates has less interference with the redox capacity of catalyst and retains part of the redox capacity. Thus, the activity in medium temperature range increases sharply. Nevertheless, NH_3 adsorption over surface sulfates at high temperatures is not strong enough, and retained redox capacity can still oxidize NH_3 at temperature as high as 450 °C, resulting in competitive reaction and performance degradation. For S-CeO_2–72h, the redox capacity is largely disturbed by bulk sulfates, which greatly restricts the catalytic performance at medium temperatures. However, the adsorption capacity for NH_3 is significantly enhanced at high temperatures, and poor oxidation capacity also reduces the competitive reaction of ammonia oxidation, which exhibits attractive catalytic activity at high temperatures.

Declaration of competing interest

The authors declare that they have no known competing financial interests or personal relationships that could have appeared to influence the work reported in this paper.

Acknowledgments

The financial supports from the National Natural Science Foundation of China (Nos. 21976081, 21972062) and Major Scientific and Technological Project of Bingtuan (No. 2018AA002), are greatly acknowledged.

Supplementary materials

Information about detailed experiment details, test conditions, quantitative result of TG profiles, composition of commercial V_2O_5-WO_3/TiO_2, compared catalysts reported in literature, integral result of NH_3-TPD, N_2-sorption, TG, XRD, H_2-TPR, SCR reaction test over commercial V_2O_5-WO_3/TiO_2, N_2 selectivity of NH_3 oxidation are in Supplementary material. Supplementary material associated with this article can be found, in the online version, at doi:10.1016/j.cclet.2022.107769.

References

[1] K. Zhao, X. Sun, C. Wang, et al., Chin. Chem. Lett. 32 (2021) 2963–2974.
[2] J. Lai, I. Wachs, ACS Catal. 8 (2018) 6537–6551.
[3] Q. Xu, Z. Fang, Y. Chen, et al., Environ. Sci. Technol. 54 (2020) 2530–2538.
[4] D. Meng, Q. Xu, Y. Jiao, et al., Appl. Catal. B 221 (2018) 652–663.
[5] W. Song, J. Ji, K. Guo, et al., Chin. Chem. Lett. 33 (2022) 935–938.
[6] C. He, R. Sun, L. Fu, et al., Chin. Chem. Lett. 33 (2022) 527–532.
[7] W. Shan, Y. Geng, X. Chen, et al., Catal. Sci. Technol. 6 (2016) 1195–1200.
[8] L. Han, M. Gao, C. Feng, L. Shi, D. Zhang, Environ. Sci. Technol. 53 (2019) 5946–5956.
[9] J. Ji, Y. Tang, L. Han, et al., Chem. Eng. J. 445 (2022) 136530.
[10] D. Meng, W. Zhan, Y. Guo, et al., ACS Catal. 5 (2015) 5973–5983.
[11] H. Chang, L. Ma, S. Yang, et al., J. Hazard. Mater. 262 (2013) 782–788.
[12] Y. Yu, X. Yi, J. Zhang, et al., Catal. Sci. Technol. 11 (2021) 5125–5134.
[13] Y. Yu, J. Zhang, C. Chen, et al., New J. Chem. 44 (2020) 13598–13605.
[14] R. Xie, L. Ma, K. Sun, et al., J. Hazard. Mater. 420 (2021) 126545.
[15] Z. Lian, W. Shan, M. Wang, H. He, Q. Feng, J. Environ. Sci. 79 (2019) 273–279.
[16] R. Xie, L. Ma, Z. Li, et al., ACS Catal. 11 (2021) 13119–13139.
[17] L. Ma, C. Seo, M. Nahata, et al., Appl. Catal. B 232 (2018) 246–259.
[18] T. Gu, Y. Liu, X. Weng, H. Wang, Z. Wu, Catal. Commun. 12 (2010) 310–313.
[19] S. Yang, Y. Guo, H. Chang, et al., Appl. Catal. B 136-137 (2013) 19–28.
[20] J. Chen, W. Zhao, Q. Wu, et al., Chem. Eng. J. 382 (2020) 122910.
[21] L. Zhang, W. Zou, K. Ma, et al., J. Phys. Chem. C 119 (2015) 1155–1163.
[22] L. Zhang, L. Li, Y. Cao, et al., Appl. Catal. B 165 (2015) 589–598.
[23] P. Loof, B. Kasemo, L. Bjornkvist, S. Andersson, A. Frestad, Stud. Surf. Sci. Catal. 71 (1991) 253–274.
[24] J. Twu, C. Chuang, K. Chang, C. Yang, K. Chen, Appl. Catal. B 12 (1997) 309–324.
[25] M. Waqif, P. Bazin, O. Saur, et al., Appl. Catal. B 11 (1997) 193–205.
[26] T. Luo, J. Vohs, R. Gorte, J. Catal. 210 (2002) 397–404.
[27] C. Tang, H. Zhang, L. Dong, Catal. Sci. Technol. 6 (2016) 1248–1264.
[28] L. Han, S. Cai, M. Gao, et al., Chem. Rev. 119 (2019) 10916–10976.
[29] Q. Xie, Y. Cai, L. Zhang, et al., J. Phys. Chem. C 125 (2021) 21964–21974.
[30] Q. Wu, X. Chen, J. Mi, et al., ACS Sustain. Chem. Eng. 9 (2021) 967–979.
[31] J. Ji, M. Jing, X. Wang, et al., J. Catal. 399 (2021) 212–223.
[32] W. Tan, J. Wang, S. Yu, et al., Top. Catal. 63 (2020) 932–943.